

# Numerical modelling of acoustic wave propagation through a bubble column

Tom A Smith<sup>1</sup>, Nikolaos Bempedelis<sup>2</sup>, and Andrea Grech La Rosa<sup>1</sup>

<sup>1</sup>University College London

<sup>2</sup>Imperial College London

Corresponding author: Tom Smith, Department of Mechanical Engineering, University College London, London, WC1E 7JE, United Kingdom. Email tom.smith.17@ucl.ac.uk

**Abstract:** *Understanding the propagation of an acoustic wave through a region of bubbles has a number of applications in underwater acoustics including the analysis of bubble screen performance. Used to reduce the impact of high amplitude acoustic sources, bubble screens are used during offshore wind turbine installation and also have the potential to reduce noise from shipping. Computational modelling of acoustic wave propagation through a bubble screen is challenging due to the relatively high void fractions and the multiple interactions that take place between the incident acoustic wave and the bubbles. In this work, a multiphase approach is applied to this problem, where the Euler equations are solved numerically for both the liquid and gas phases, with a Lagrangian front-tracking technique to capture the interface. A series of simulations are conducted with different random distributions of bubbles and different void fractions, and the results show that a transmission coefficient of less than 0.01 can be achieved for a void fraction of 3%. It is also shown that the distribution of the bubbles plays a significant role in determining the transmission coefficient. For different spatial distributions of a fixed number of bubbles within a fixed area, the highest transmission coefficient is found to be 4 times higher than the lowest, highlighting the importance of properly accounting for the location of each bubble within the column.*

**Keywords:** *multiphase flows, underwater acoustics, bubbly flows, Lagrangian front-tracking*

## 1. INTRODUCTION

The propagation of acoustic waves through a bubbly liquid has a number of practical applications in underwater acoustics, including in oceanography, the use of sonars for detection and mapping, and also bubble screens. Bubble screens are devices used to reduce the transmission of very loud acoustic sources such as those produced by pile driving and explosives and shock testing [1] in order to protect marine life. There has also been renewed interest in recent years in using bubble screens on ships to reduce the propagation of machinery and propeller noise. Bubble screens reduce acoustic transmission by acting as impedance barriers and through induced oscillations of the bubbles by the acoustic wave [2, 3]. In theory, a relatively low void fraction can lead to very low transmission coefficients, but field trials of existing designs often show only very modest reductions in radiated noise [1, 4], which shows further research is needed into their design, operation, and performance.

Numerical and analytical models need to be able to capture a number of complex phenomena in order to accurately determine how an acoustic wave will propagate through a bubble screen. Despite decades of research into the modelling of wave propagation through bubbly flows, it is noted by [5] that agreement between models and experiments is often poor, particularly for frequencies close to resonance and for larger void fractions. In a recent study [6], it was shown that bubble screens typically have void fractions of around 1% and at these levels bubble-bubble interactions are expected to be significant [5]. To enable more practical computations, many approaches neglect these interactions [7] but a lack of detailed parametric data, either from experiments or high fidelity simulations, makes it difficult to quantify the effect of including or neglecting such phenomena. Another important effect is shielding, where upstream bubbles affect the interaction between the incident wave and bubbles further downstream. This has been shown to be significant on the overall transmission of a wave through a column of bubbles [8] and so should be included in any modelling. Another consideration is the amplitude and linearity of the incident wave. For low amplitude linear acoustic waves, a linear spherical bubble response may be assumed, but for very high acoustic amplitudes or shock waves, a non-linear response or a bubble collapse can occur [9]. Therefore, we seek a model that can accurately account for interactions between multiple bubbles and an incident wave, bubble-bubble interactions, shielding effects, and potential non-linearities depending on the nature of the incident wave.

In this work, a direct numerical approach is used to model the propagation of an acoustic wave through a column of bubbles. The Euler equations are solved for both the liquid and gas phases, and a Lagrangian front-tracking model is used to resolve the bubble surface. This approach removes the need for any additional modelling and places no restrictions on the shape or dynamics of the bubbles. A series of parametric simulations are conducted to investigate the effect of changing void fraction, bubble column width, and the distribution of bubbles on the transmission of an acoustic pulse. To capture the stochastic nature of a bubble screen, different random distributions are considered to better understand the variability in transmission that occurs as a result of the spacing and clustering of the bubbles. As well as providing insights into the propagation of acoustic waves through high void fraction bubble columns, these high fidelity simulations will also allow for lower-order and more computationally efficient methods to be validated for different configurations.

Set	Void fraction, $v_B$	Column width, $b$ (m)	Random distribution	Points per bubble radius
1	0.01	0.25	fixed	3, 5, 10, 15
2	0.005, 0.01, 0.02, 0.03	0.125, 0.25, 0.50	fixed	5
3	0.01	0.25	variable	5

Table 1: Description of the parameters for each set of simulations

## 2. METHODS

### 2.1. NUMERICAL METHODS

The Euler equations are solved numerically for both the liquid and gas phases. A Lagrangian front-tracking approach [10, 9] is used to capture the interface, which enables the geometry of the bubble to be captured more accurately than volume-of-fluid approaches, and allows for the bubble shape to be directly determined by the solutions to the Euler equations in both phases. This approach has been validated for a range of bubble-wave interaction problems in two and three dimensions including shock-induced bubble collapse [9]. The equations are solved using a finite-difference approach, with spatial discretisation being performed using a 5th-order WENO approach. Explicit time-stepping is performed using a strong stability preserving 3rd-order Runge-Kutta method. Time steps are chosen to ensure a Courant number of less than 0.5.

The bubbles are generated using a uniform random distribution for the x- and y-coordinates of the centroids. Different seed values can be chosen to generate different random distributions. The number of bubbles for each simulation is determined by the void fraction  $v_B$ , the column width  $b$  and the bubble radius  $r$ . To reduce the number of parameters, the bubble radius is kept constant at  $r = 0.005\text{m}$ , which is a typical radius for a bubble screen application [4]. The bubbles are in equilibrium at time  $t = 0$  and so are not oscillating. This has been done to allow for the bubble response to the incident wave to be more directly captured.

### 2.2. PROBLEM DEFINITION

The simulations are conducted on a 2D domain with a single acoustic wave propagating initially from left to right. A column of randomly distributed bubbles is located in the middle of the domain, as shown in figure 1. The top and bottom boundaries are periodic, and so waves are mapped between the two according to their direction, and the left and right boundaries are modelled as non-reflecting flow-through conditions. The initial condition consists of a sinusoidal pulse with an amplitude of 1kPa and a wavelength of  $\lambda = 0.5\text{m}$ . The pulse is initialised upstream of the bubble column, as shown in figure 1. The initial pressure field is used to determine the initial velocity and density values by solving the linearised Euler equations. The wavelength and amplitude of the incident wave are fixed in this study, partly to reduce the number of variables and also to focus on the impact of changing the bubble screen parameters.

3 sets of simulations have been set up and are described in table 1. For many practical applications, the acoustic wavelength will be a similar order of magnitude or longer than the

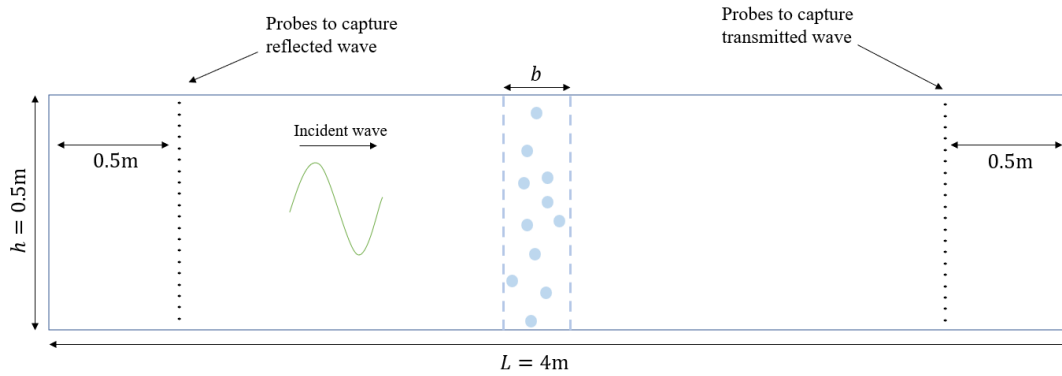


Figure 1: Illustration of the computational domain.

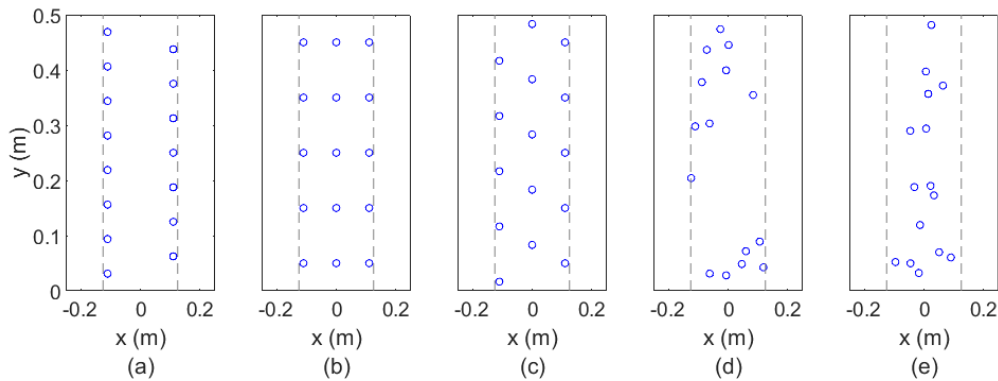


Figure 2: Illustration of 5 different bubble distributions: (a) 2-column distribution, (b) 3-column in-line, (c) 3-column offset, (d-e) random distributions.

bubble screen width, and so the bubble column width is  $b \leq \lambda$  for all of the cases considered. The first set of simulations is a grid sensitivity study designed to determine the number of points needed to capture the necessary fluid dynamics. Grid resolutions commensurate with 3, 5, 10 and 15 points per bubble radius (ppbr) are considered, leading to grids with  $(N_x \times N_y) = (2400 \times 300), (4000 \times 500), (8000 \times 1000), (12000 \times 1500)$  points. The second set varies the void fraction and bubble screen width. Here, the random distribution is kept constant to allow for a more direct comparison between the simulations in this set. Set 3 has the same void fraction and column width as set 1, but uses different random distributions of bubbles. Alongside 30 random bubble arrays, three additional arrays are used where the bubbles are in specific configurations, as shown in figure 2(a-c). The first of these consists of two separate columns of evenly spaced bubbles at  $y = \pm 0.12\text{m}$ . The second has three equally spaced columns to allow for the effect of shielding to be examined and the third has three columns which are offset in the y-direction so that no bubble directly shields another. The two random distributions shown in figure 2(d-e) represent the two extremes for the 30 distributions, as will be shown in the following section.

### 3. RESULTS

Figure 3 shows the pressure field at 3 points in time, before, during, and after the incident wave has interacted with the bubble array. The case shown is for a void fraction of 0.01 and a width

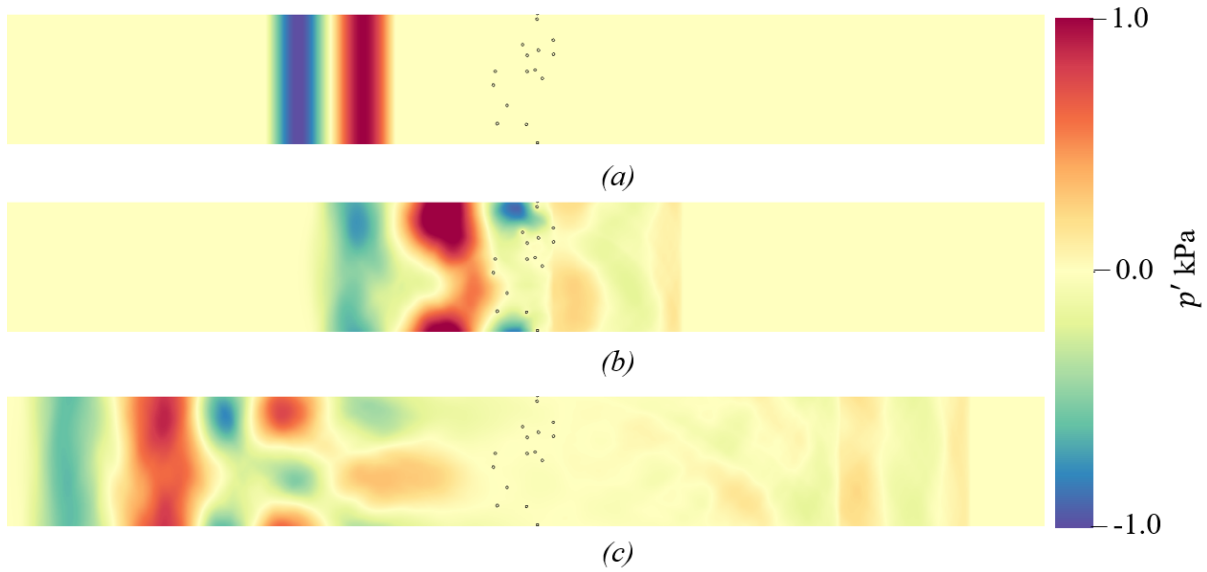


Figure 3: Contour plots of the pressure fluctuation at (a)  $t = 0s$ , (b)  $t = 0.00075s$ , and (c)  $t = 0.0015s$

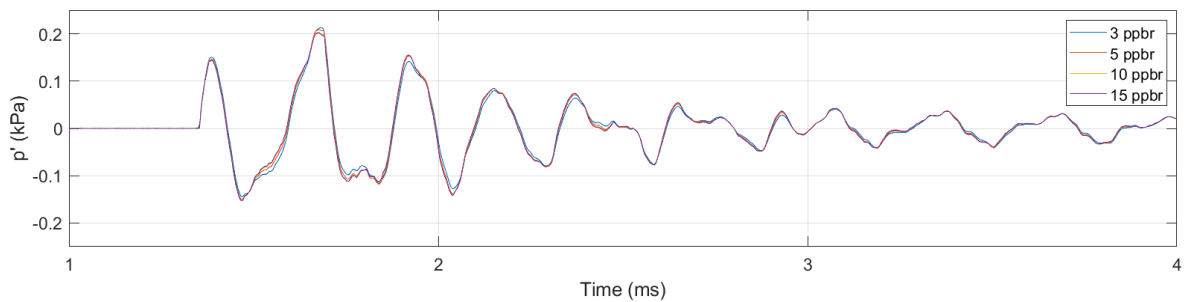


Figure 4: Comparison of the pressure fluctuations at a probe of the bubble array downstream for the four different grid resolutions.

of 0.25m, and is taken from simulation set 3. It is clear from this that only a small portion of the incident wave is transmitted through the bubble array and that the spatial distribution of the bubbles is likely to be significant.

To demonstrate the grid independence of the results, figure 4 shows the pressure downstream of the bubble screen at  $y = 0.5$ . The pressure is shown for a duration of 3ms, starting just before the transmitted wave arrives at the probes. The overall agreement between the 4 simulations is excellent, although there is some disagreement between the coarsest grid and the three finer grids. The results from the finer three grids are in good agreement and so all subsequent simulations have been conducted with a resolution of 5 points per bubble radius.

Figure 5 shows the transmission coefficient for the bubble arrays with varying void fraction and array width. Due to the acoustic source being a single sine wave, the transmission coefficient has been computed using the maximum peak-to-trough difference for all downstream probes and then taking an average of these. As one would expect, the transmission drops with increasing void fraction and with increasing width, both of which increase the total number of

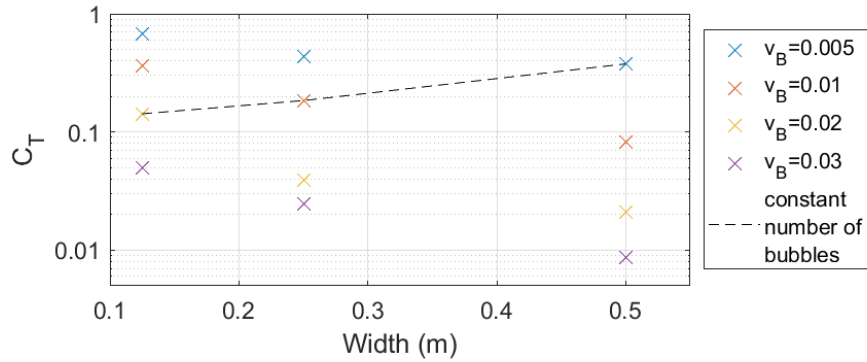


Figure 5: Transmission coefficients for varying void fractions and bubble screen widths

bubbles. For the highest void fraction and widest screen, the transmission coefficient is 0.0086, equivalent to a reduction of 41dB, which demonstrates how effective bubble screens can be if this level of void fraction can be achieved. It can also be seen that, for a constant number of bubbles, the transmission coefficient decreases with decreasing width showing that for a fixed air supply it is favourable to try and design the screen so that the lateral spread of the bubbles is as low as possible.

To investigate the variability of the transmission coefficient for a fixed void fraction and column width, 30 random distributions and the 3 additional distributions shown in figure 2 have been computed. For the 30 random distributions, the mean transmission coefficient is  $C_T = 0.183$ , but the range is quite large:  $0.109 < C_T < 0.322$ . The maximum transmission occurs of the distribution shown in figure 2(d) and the minimum occurs for the (e). The bubbles for (d) are mostly clustered in two groups, with a region in the middle with a much lower effective void fraction. For (e), the bubbles are more spread out in the y-direction, providing a more effective impedance barrier for the acoustic wave. For the 3 non-random arrays, the transmission coefficients are 0.079 for the 2-column array, 0.126 for the 3-column in-line array and 0.119 for the 3-column offset array. These are all lower than the mean coefficient for the 30 random arrays, implying that more equal spacing and lack of bubble clusters is beneficial. The closeness of the coefficients for the three-column distributions implies that shielding is having only a limited impact here, probably due to the large spacing between three columns relative to the bubble radii. What these results clearly show is that the distribution of bubbles within the column plays a very important role in determining the transmission properties. This helps to explain the intermittent performance that has been observed in experimental tests of bubble screens [11], where the transmission properties are shown to vary significantly over short time periods, which is attributed to bubble interactions leading to local variations in the bubble concentrations in the screen.

#### 4. CONCLUSIONS

In this work, a multiphase front-tacking solver has been used to investigate acoustic wave propagation through a column of randomly distributed bubbles. The effect of void fraction, column width, and distribution of bubbles on the transmission coefficient has been assessed. It has been shown that transmission coefficients less than 0.01 can be obtained for a void fraction of  $v_B = 0.03$  and that for a given number of bubbles it is favourable to have a narrow column of

equally spaced bubbles to achieve the lowest transmission. Future work is planned to consider a larger parametric study with both transient and continuous noise sources. This larger study will allow for variations in incident wavelength and amplitude, bubble radius, and bubble columns containing a distribution of bubble sizes. Bubbles that are freely oscillating will also be considered to better understand how this affects the transmission and interaction with the incident acoustic wave.

## 5. ACKNOWLEDGEMENTS

The Authors wish to acknowledge the use of the UCL Kathleen High Performance Computing Facility and associated support services in the completion of this work.

## REFERENCES

- [1] B Würsig, CR Greene Jr, and TA Jefferson. Development of an air bubble curtain to reduce underwater noise of percussive piling. *Marine environmental research*, 49(1):79–93, 2000.
- [2] V Leroy, A Strybulevych, MG Scanlon, and JH Page. Transmission of ultrasound through a single layer of bubbles. *The European Physical Journal E*, 29(1):123–130, 2009.
- [3] K M Lee, P S Wilson, and M S Wochner. Attenuation of standing waves in a large water tank using arrays of large tethered encapsulated bubbles. *The Journal of the Acoustical Society of America*, 135(4):1700–1708, 2014.
- [4] T Bohne, T Griebmann, and R Rolfes. Modeling the noise mitigation of a bubble curtain. *The Journal of the Acoustical Society of America*, 146(4):2212–2223, 2019.
- [5] D Fuster, J-M Conoir, and T Colonius. Effect of direct bubble-bubble interactions on linear-wave propagation in bubbly liquids. *Physical Review E*, 90(6):063010, 2014.
- [6] S Beelen, M van Rijsbergen, M Birvalski, F Bloemhof, and D Krug. In situ measurements of void fractions and bubble size distributions in bubble curtains. *Experiments in Fluids*, 64(2):31, 2023.
- [7] A Tsouvalas and AV Metrikine. Noise reduction by the application of an air-bubble curtain in offshore pile driving. *Journal of Sound and Vibration*, 371:150–170, 2016.
- [8] A Madabhushi and K Mahesh. A compressible multi-scale model to simulate cavitating flows. *Journal of Fluid Mechanics*, 961:A6, 2023.
- [9] N Bempedelis and Y Ventikos. A simplified approach for simulations of multidimensional compressible multicomponent flows: The grid-aligned ghost fluid method. *Journal of Computational Physics*, 405:109129, 2020.
- [10] J Glimm, E Isaacson, D Marchesin, and O McBryan. Front tracking for hyperbolic systems. *Advances in Applied Mathematics*, 2(1):91–119, 1981.
- [11] A Grech La Rosa and T A Smith. An experimental parametric study on bubble screen performance. In *Underwater Acoustics Conference and Exhibition Series 2023*, 2023.

